Point Contact Conductance of an Open Resonator

J. A. Katine,* M. A. Eriksson, A. S. Adourian, and R. M. Westervelt
Division of Applied Sciences and Department of Physics, Harvard University, Cambridge, Massachusetts 02138

J. D. Edwards, A. Lupu-Sax, and E. J. Heller
Department of Physics and ITAMP, Harvard University, Cambridge, Massachusetts 02138

K. L. Campman and A. C. Gossard
Materials Department, University of California-Santa Barbara, Santa Barbara, California 93106
(Received 20 June 1997)

Coherent resonant tunneling peaks are observed in the conductance of a quantum point contact coupled to an *open* resonator in a two-dimensional electron gas as we tune the resonator's dimensions. A wavelet based boundary wall method is used to compute both the electronic wave function and probability current in and around the resonator. We find excellent agreement between the calculated and measured conductance resonances, and identify fine structure associated with the lemon billiard cavity modes. [S0031-9007(97)04837-0]

PACS numbers: 73.23.Ad, 05.45.+b, 73.40.Gk

Recent experiments on two-dimensional electron gas (2DEG) systems have examined the effect that the shape of a quantum billiard can have on its electronic transport properties. For example, the power spectrum of magnetoconductance fluctuations [1,2] as well as the line shape of the weak localization peak [3] both show a clear distinction between devices whose boundary shapes are classically chaotic and those whose shapes are classically integrable. In related work [4] scarred chaotic orbits are found to enhance the conductance of resonant tunnel diodes. The results of these experiments have provided a test of semiclassical theory, which assumes electrons carry phase while moving along classical trajectories [5]. Although it is possible to discern some information about individual orbits in these experiments [3,6], they measure the entire ensemble of electron trajectories present in the billiards. As a result, it has only been possible to experimentally examine the statistical predictions of semiclassical theory.

Much of the interest in quantum billiards, however, centers on individual trajectories. For example, the wave function of a classically chaotic system may be scarred by the remnants of a small number of periodic orbits [7]. In this Letter, we describe coherent resonant tunneling measurements in an open electrostatically tunable resonator. These measurements provide a means of examining the effect of individual cavity modes on the transport properties of the device. When the conductance of a quantum point contact (QPC) is tuned in the tunneling regime so that less than one transverse mode is transmitted, the presence of nearby scattering sources can lead to dramatic interference effects, as in recent experiments on quantum dot edge states [8,9]. Unlike tunneling experiments into quantum dot edge states, our measurements are performed in zero field, so we probe ballistic electron trajectories. An even more important distinction is that our resonator is *open*, so the quantum states form a continuous spectrum and tunneling occurs into the stable (nonchaotic) modes of the resonator. We have developed a wavelet based technique that readily allows us to compute the electronic wave function and the resulting conductance of an arbitrary two-dimensional structure. When a realistic amount of damping is included, we find excellent agreement between these calculations and our experimental measurements, which enables us to identify the modes of our resonator associated with each observed conductance peak.

Figure 1 is a scanning electron microscopy (SEM) photograph of the central region of the device. The bright regions are Cr/Au gates patterned on the surface of the $GaAs/Al_xGa_{1-x}As$ heterostructure using electron-beam lithography followed by thermal evaporation. The 2DEG lies 470 Å beneath the surface and has a low temperature mean free path of 5.0 μm. The electronic sheet density $3.5 \times 10^{15}\ \mathrm{m}^{-2}$ corresponds to a Fermi wavelength $\lambda_F = 42$ nm. The reflector gates are circular arcs, 800 nm radius of curvature, centered on the QPC. Although two reflector gates are present, only one is energized, so the resonant cavity consists of the point contact and that single reflector gate. As shown in the circuit schematic included with Fig. 1, the gate voltages applied to the point contact and the two reflectors are independently tunable. As a reproducibility check, the roles of the two reflectors were reversed [10]. In addition, measurements were performed on a device where the circular mirrors were replaced by plunger gates with 300 nm long flat surfaces located 500 nm from the QPC.

Reflection from electrostatically defined gates is predominantly specular [11], allowing the circular mirror to focus injected electrons back to the point contact. Hence, the device shown in Fig. 1 is a concentric open resonator. If we move the reflector gate towards the QPC, the circular symmetry of our cavity is lost, creating an open lemon

 0031-9007/97/79(24)/4806(4)$10.00

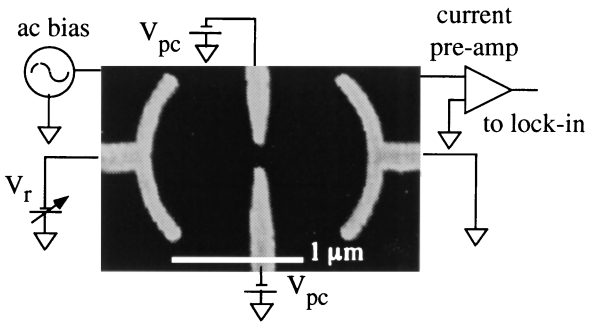

FIG. 1. SEM photo of the device including a measurement circuit schematic. Only one reflector is depleted at a time. By varying V_r, the reflector-QPC spacing in the 2DEG can be adjusted.

billiard [12]. Experimentally this can be accomplished by increasing the magnitude of the negative bias applied to the reflector gate. Doing so extends the boundary of the depleted 2DEG regions towards the QPC. A similar technique was used in earlier electron interferometry experiments [13]. Even though our resonator has rather substantial gaps in its boundary, it is still possible to achieve long dwell times for electrons within it. The geometry is such that most of the injected electrons are trapped in a "phase space bottle," since the classical modes of our resonator are stable and remain confined, except for the hole at the point contact. If the point contact is sufficiently narrow, escape from the cavity through simple classical backscattering is strongly suppressed, allowing sharp conductance resonances to be observed as we tune the dimensions of the cavity.

Holding the QPC at a fixed negative bias, the conductance of the device is measured as the voltage V_r applied to one of the reflector gates is ramped. A voltage-biased lock-in technique (10 μV excitation, 11 Hz) is used to measure the device conductance. The samples are cooled in a dilution refrigerator, and unless noted otherwise, all measurements are made at a sample temperature of 100 mK. Figures 2(a)–2(c) display the device conductance as a function of reflector bias V_r with the point contact potential V_{pc} held at three successively lower conductance values in the tunneling regime. Between $V_r = 0$ and $V_r = 0.35$ V, the electron gas beneath the reflector gate has yet to be fully depleted. Following depletion at $V_r \cong -0.35$ V, strong enhancement peaks in the device conductance are observed as the result of coherent resonant tunneling into the open resonator. Figure 2(d) is a curve obtained from the device with the flat plunger. The oscillations immediately following depletion for the flat plunger are not as simple or strong as for the curved resonator, because focusing by the curved mirror is more forgiving to disorder [14].

It is interesting to note that the conductance through the QPC sometimes *increases* when the concentric mirror is introduced. We have approached this problem in the

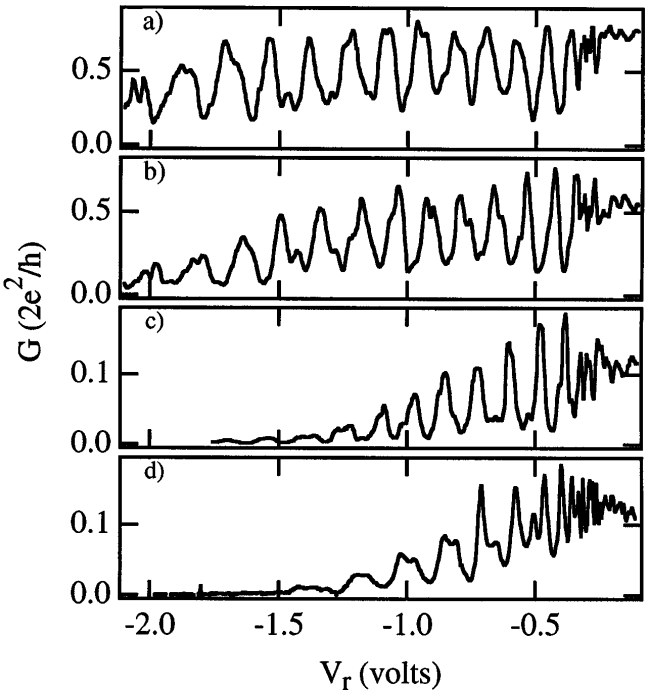

FIG. 2. As V_{pc} is held at three successively more negative values (a)–(c), conductance peaks associated with coherent resonant tunneling are evident at certain reflector bias voltages. In (c) we clearly see that the average device conductance is being reduced by increasing the bias on the reflector gate. Curve in (d) obtained from device with flat plunger gate.

spirit of the Landauer-Büttiker scattering theory [15]. To this end, we treat the QPC as an absorptive point scatterer embedded in a line which is otherwise completely reflective. In the lowest partial wave expansion, including averaging over incoming states and summing over both spins, we find that the maximum conductance, corresponding to flux loss on the incident side is $2e^2/h$, *independent of the size of the QPC* in the small QPC limit [16]. In agreement with this scattering theory, the experimental conductance is enhanced at resonances in Figs. 2(b) and 2(c), and approaches, but never exceeds, $2e^2/h$.

Figure 2(c) clearly illustrates that the average conductance of devices in the tunneling regime decreases monotonically as a more negative bias is applied to the reflector. This is a "cross talk" effect. In the tunneling regime, the conductance of the QPC is very sensitive to nearby potentials, and the reflector gate is close enough that the negative reflector bias pinches down the QPC. It is possible to remove this effect by normalizing the data to a smooth background conductance $G_0(V_r)$ obtained by repeating the trace at a temperature of 4.2 K where the quantum interference phenomena are suppressed. In Fig. 3(a), we replot the data from Fig. 2(c) using this normalization procedure.

In order to understand which cavity modes are responsible for the observed conductance resonances, we performed numerical calculations of the conductance, as well as of the wave functions inside the cavity, using a wavelet

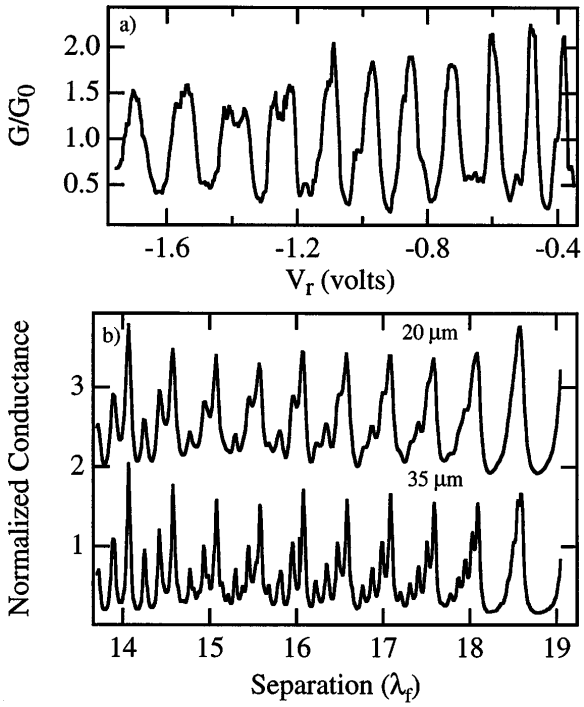

FIG. 3. (a) Experimental conductance trace of Fig. 2(c), normalized to remove cross-talk effect. (b) Normalized conductance of our cavity calculated with 20 μm (upper) and 35 μm (lower) dephasing lengths; offset for clarity.

based boundary wall method [17]. Wavelets allow us to use a fine resolution when it is necessary, such as when computing the multiple scattering between the tips of the QPC, and a coarser resolution when computing the interaction of two well separated segments of the cavity walls. Because the derivative of the two-dimensional free space Green's function is a known analytic function, both the wave function and its derivative can be computed with the boundary wall method, and the probability current is readily calculated. The conductance is found by integrating the normal component of the current across a theoretical "detector" placed in the QPC.

In Fig. 3(b) we plot the conductance of our resonator calculated as a function of the separation between the point contact and the reflector [18]. In order to facilitate comparison with the experimental data in Fig. 3(a), we present the results of our calculations in normalized form. The largest amplitude conductance peaks in Fig. 3(b) are periodic with spacing equal to $\lambda_F/2$. These conductance peaks are associated with the simplest stable modes of our resonator, analogous to those of a one-dimensional interferometer; the wave functions of these modes have their maxima along the central axis of the resonator, and there are no angular nodes. Comparing the experimental and theoretical conductance traces in Fig. 3, we see excellent agreement in that both are dominated by these $\lambda_F/2$ periodic oscillations. In order to align the calculated and experimental conductances, one need only assume a linear relationship ($dL/dV_r = 160$ nm/V) between the applied gate voltage V_r and the distance L moved by the mirror; such a linear relationship is consistent with the nearly constant gate/electron gas capacitance calculated and observed for similar systems [19].

The coherence time of an electron in a classically closed orbit within the resonator is finite. The resulting damping has been introduced into the calculated conductance traces of Fig. 3(b) by continuing the free space Green's function into the complex energy plane by an amount equal to 2π divided by the coherence length $l_\phi = v_F \tau_\phi$. The upper and lower traces in that figure correspond to coherence lengths of $l_\phi = 20$ μm and $l_\phi = 35$ μm, respectively. In addition to the dominant $\lambda_F/2$ periodic oscillations, smaller amplitude conductance peaks are also evident in Fig. 3(b). These result from more complex stable modes supported in our resonator. As in the lemon billiard [12,17], these modes possess higher order angular structure, in which the electronic wave function has an even number of angular nodes. Each of these modes produces conductance oscillations with a different period, producing the peak splitting evident in the conductance traces shown in Fig. 3(b). Though not pictured in Fig. 3(b), in the absence of damping our calculated conductance exhibits extremely sharp Fano resonances, where all of the modes of the resonator appear as distinct conductance peaks. Shortening the phase coherence length smears these closely spaced resonances together, producing broad peaks with fine structure from the remnants of the individual modes. As shown in Fig. 3(a), we observe similar reproducible fine structure in our experimental measurements. This structure suggests that our coherent resonant tunneling measurement is sensitive to these complex stable modes, but that the damping present in our experimental system prevents us from clearly resolving them from the dominant $\lambda_F/2$ periodic modes of our device.

A number of factors contribute to damping in our resonator. When the quantum point contact is sufficiently wide, our experimental conductance resonances are broadened by backscattering through the point contact. We see in Figs. 2(a) and 2(b) that the half-width of the first five conductance peaks following depletion drops from 32 to 26 mV as we constrict the width of the point contact. Eventually, however, we reach a point where further constriction of the QPC has almost no effect on these half-widths, indicating that experimental limitations inherent to gated 2DEG devices rather than backscattering through the QPC are now the dominant source of broadening in the resonator. Examples of such limitations include elastic impurity scattering in the 2DEG, nonspecular boundary scattering, and distortions in the shape of the boundary potential as it is translated from the surface gate to the 2DEG. In a closed cavity, one would not expect the disorder introduced by elastic scattering to broaden the conductance resonances. However, we have an open cavity

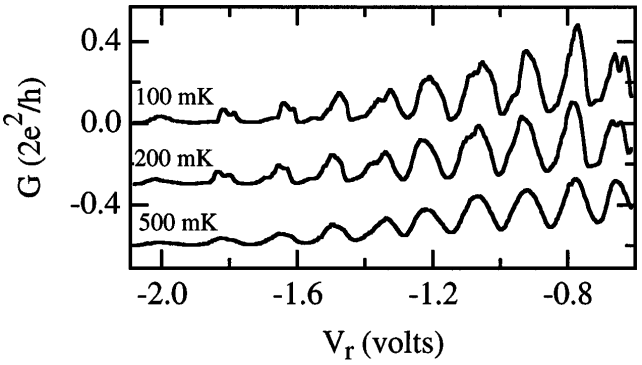

FIG. 4. The amplitude of the resonance peaks decays as the temperature is increased from 100 to 500 mK. Also note that the fine structure present in the curves disappears with increasing temperature. Curves offset for clarity.

in which long electron dwell times are only possible when electrons are trapped inside. Elastic scattering events can facilitate escape from the device, effectively broadening the experimental resonances.

An intrinsic source of damping is the finite electronic phase coherence length. At low temperature, dephasing is dominated by inelastic electron-electron scattering. For a zero-dimensional cavity such as ours, we know of no calculation for the inelastic scattering time τ_ϕ, but experimental measurements performed with quantum dots in 2DEGs very similar to our own show τ_ϕ to be approximately 150 ps at 100 mK [20,21]. When multiplied by the Fermi velocity 2.5×10^5 m/s, these measurements correspond to a ballistic dephasing length of 35 μm. Experimentally, it is possible to shorten the phase coherence time by increasing the temperature. In Fig. 4, we show conductance traces repeated at 100, 200, and 500 mK. According to the experiments of Clarke *et al.* [20] l_ϕ at 200 mK is greater than 20 μm, and is still about 10 μm at 500 mK. Hence, the decrease in amplitude of our conductance resonances as the temperature is raised from 100 to 500 mK is evidence that some electrons experience a dozen or more reflections within the device before escaping, despite the action of impurity scattering. The presence of such stable orbits in our open resonator is further evidence that we have been able to focus ballistic electron trajectories via reflection from electrostatic boundaries. Such focusing techniques may be a useful tool for those interested in "electron optics" [22]. We also see in Fig. 4 that the fine structure present in our conductance traces is attenuated as the temperature is raised. This behavior is consistent with our earlier speculation that this fine structure is due to coherent resonant tunneling into the stable resonant modes with higher order angular structure; as the phase coherence length decreases, our calculations show that any signatures of such modes are washed out, leaving only broad, periodic conductance oscillations like those observed in the 500 mK trace.

The authors wish to thank C. M. Marcus and D. C. Ralph for discussions. This work was funded at Harvard by ONR Grants No. N00014-95-1-0104 and No. N00014-95-0866 and NSF Grants No. CHE-9321260 and No. PHY94-071, and at UCSB by AFOSR Grant No. F49620-94-1-0158.

*Present address: School of Applied and Engineering Physics, Cornell University, Ithaca, NY 14853.

[1] C. M. Marcus *et al.*, Phys. Rev. Lett. **69**, 506 (1992).
[2] M. J. Berry *et al.*, Phys. Rev. B **50**, 17 721 (1994).
[3] A. M. Chang *et al.*, Phys. Rev. Lett. **73**, 2111 (1994).
[4] P. B. Wilkinson *et al.*, Nature (London) **380**, 608 (1996).
[5] R. A. Jalabert, H. U. Baranger, and A. D. Stone, Phys. Rev. Lett. **65**, 2442 (1990).
[6] J. P. Bird *et al.*, Europhys. Lett. **35**, 529 (1996).
[7] E. J. Heller, Phys. Rev. Lett. **53**, 1515 (1984).
[8] B. J. Van Wees *et al.*, Phys. Rev. Lett. **62**, 2523 (1989).
[9] A. T. Johnson *et al.*, Phys. Rev. Lett. **69**, 1592 (1992).
[10] For example, Figs. 2 and 4 are from the same device with the roles of the two reflector gates reversed. Similar results were obtained in lithographically identical devices.
[11] T. J. Thornton *et al.*, Phys. Rev. Lett. **63**, 2128 (1989).
[12] E. J. Heller and S. Tomsovic, Phys. Today **46**, No. 7, 38 (1993).
[13] C. G. Smith *et al.*, J. Phys. Condens. Matter **1**, 9035 (1989).
[14] The distinction is even more dramatic considering the smaller lithographic separation between the plunger and QPC should help mitigate scattering effects.
[15] R. Landauer, IBM J. Res. Dev. **1**, 223 (1957); M. Büttiker, Phys. Rev. Lett. **57**, 1761 (1986).
[16] A. S. Lupu-Sax *et al.* (to be published).
[17] J. D. Edwards and E. J. Heller (to be published).
[18] This calculation assumes that the shape of the reflector is preserved as the QPC/reflector spacing decreases.
[19] D. B. Chklovskii, B. I. Shklovskii, and L. I. Glazman, Phys. Rev. B **46**, 4026 (1992); F. R. Waugh *et al.*, Phys. Rev. B **53**, 1413 (1996).
[20] R. M. Clarke *et al.*, Phys. Rev. B **52**, 2656 (1995).
[21] J. P. Bird *et al.*, Phys. Rev. B **51**, 18 037 (1995).
[22] J. Spector *et al.*, Surf. Sci. **263**, 240 (1992).